Noncovalent functionalization of carbon nanotubes for highly specific electronic biosensors

Robert J. Chen*, Sarunya Bangsaruntip*, Katerina A. Drouvalakis†, Nadine Wong Shi Kam*, Moonsub Shim*, Yiming Li*, Woong Kim*, Paul J. Utz†, and Hongjie Dai*‡

*Department of Chemistry, and †School of Medicine, Department of Medicine, Division of Immunology and Rheumatology, Stanford University, Stanford, CA 94305

Edited by William A. Goddard III, California Institute of Technology, Pasadena, CA, and approved February 27, 2003 (received for review November 19, 2002)

Novel nanomaterials for bioassay applications represent a rapidly progressing field of nanotechnology and nanobiotechnology. Here, we present an exploration of single-walled carbon nanotubes as a platform for investigating surface–protein and protein–protein binding and developing highly specific electronic biomolecule detectors. Nonspecific binding on nanotubes, a phenomenon found with a wide range of proteins, is overcome by immobilization of polyethylene oxide chains. A general approach is then advanced to enable the selective recognition and binding of target proteins by conjugation of their specific receptors to polyethylene oxide-functionalized nanotubes. This scheme, combined with the sensitivity of nanotube electronic devices, enables highly specific electronic sensors for detecting clinically important biomolecules such as antibodies associated with human autoimmune diseases.

Recent years have witnessed significant interest in biological applications of novel inorganic nanomaterials such as nanocrystals (1, 2), nanowires (3), and nanotubes (4, 5) with the motivation to create new types of analytical tools for life science and biotechnology. Single-walled carbon nanotubes (SWNTs) are interesting molecular wires (diameter ≈1–2 nm) with unique electronic properties that have been spotlighted for future solid-state nanoelectronics (6, 7). Bridging nanotubes with biological systems, however, is a relatively unexplored area, with the exception of a few reports on nanotube probe tips for biological imaging (4), nonspecific binding (NSB) of proteins (8–10), functionalization chemistry for bioimmobilization on nanotube sidewalls (5), and one study on biocompatibility (11).

Previously, we and others have shown that the electrical conductance of a nanotube is highly sensitive to its environment and varies significantly with changes in electrostatic charges and surface adsorption of various molecules (12–14). This research has hinted at possible SWNT-based miniature sensors for detecting biological molecules in fluids. Here, we systematically explore how nanotubes interact with and respond to various proteins in solution, how chemical functionalization can be used to tailor these interactions, and how the resulting understanding enables highly selective nanotube sensors for the electronic detection of proteins. Using atomic force microscopy (AFM) and quartz crystal microbalance (QCM) and electronic transport measurements, we first reveal that proteins in general exhibit a high degree of NSB on nanotubes, a phenomenon undesirable for potential biosensors. We then demonstrate a functionalization scheme involving irreversible adsorption of Tween 20 or triblock copolymer chains on nanotubes to prevent this general NSB, while at the same time enabling the binding of specific proteins of interest that can be detected electronically without the need for labeling. Further, we demonstrate specific detection of mAbs to the human autoantigen U1A, a prototype target of the autoimmune response in patients with systemic lupus erythematosus and mixed connective tissue disease.

Methods

Materials. All chemicals were purchased from Sigma-Aldrich except for Pluronic P103 (BASF Bioresearch, Cambridge, MA), biotin-long chain-polyethylene oxide (PEO)-amine (Pierce), and staphylococcal protein A (SpA) (Pierce). mAbs 6E3, 3E6, and 10E3 were kindly provided by Paul Anderson (Brigham and Women's Hospital, Harvard Medical School, Boston) and Carol Lutz (University of Medicine and Dentistry of New Jersey, Newark) and purified by protein A Sepharose chromatography. Six times his-tagged U1A antigen expressed in baculovirally infected SF9 cells and purified to homogeneity by nickel column chromatography was obtained from Diarect (Freiburg, Germany).

AFM Experiments. For AFM studies, nanotubes were grown on SiO_2 substrates by chemical vapor deposition on discrete metal-catalyst nanoparticles derived from ferritin (15). The nanotubes are single-walled with diameters ≈1–3 nm and lengths ≈1–10 μm. For studying protein NSB, as-grown samples were immersed in phosphate-buffered solutions (10 mM, pH 7.0) of each one of the proteins, streptavidin (SA), avidin, BSA, α-glucosidase, and SpA, at a concentration of 10–50 nM for 1 h. The samples were then rinsed thoroughly with water and dried with a stream of argon before AFM imaging. For NSB blocking studies, as-grown nanotube samples were first immersed in a 10 wt% water solution of each surfactant in Table 1 for 1 h, thoroughly rinsed, and then exposed to protein solutions in the same manner as above before AFM imaging.

QCM Experiments. QCM measurements were performed with a Q-Sense D-300 instrument (Q-Sense, Newport Beach, CA). Optically polished quartz crystal substrates (5 MHz, AT cut) coated with gold were used. Frequency shifts caused by mass uptake were measured at the third harmonic resonance of the crystal. A typical SWNT film was formed on a quartz crystal surface by first dispersing bulk SWNTs produced by high-pressure CO (Carbon Nanotechnologies, Houston) in chloroform at a concentration of 50 μg/ml. One hundred microliters of this suspension was then deposited onto the crystal surface dropwise and baked at 60°C for 1 h. Control experiments were done on bare QCM substrates without deposited nanotubes.

Activation of Tween 20 for Conjugation to Biotin, SpA, and U1A. Tween 20 (5.0 mg, 0.27 M) and 1,1-carbonyldiimidazole (CDI) (4.0 g, 0.81 M) were allowed to react in DMSO (25 ml, dried under molecular sieve) at 40°C for 2 h with stirring. Ethyl ether was then added to effect precipitation, after which the precipitates were collected, redissolved in DMSO, and reprecipitated in ether. This process was repeated twice to ensure the removal of excess CDI and was followed by drying the intermediate *in vacuo* overnight. For conjugation to biotin, SpA, and U1A,

This paper was submitted directly (Track II) to the PNAS office.

Abbreviations: AFM, atomic force microscopy; NSB, nonspecific binding; PEO, polyethylene oxide; QCM, quartz crystal microbalance; SA, streptavidin; SpA, staphylococcal protein A; SWNT, single-walled carbon nanotube.

‡To whom correspondence should be addressed. E-mail: hdai@stanford.edu.

www.pnas.org/cgi/doi/10.1073/pnas.0837064100

Table 1. Survey of whether various proteins bind to as-grown nanotubes and nanotubes treated with the listed molecules

Nanotubes	SA	Avidin	BSA	GCD	SpA
As-grown nanotubes	Y	Y	Y	Y	Y
Tween 20-treated	N	N	N	N	N
Pluronic P103-treated	N	N	N	N	N
Triton X-100-treated	N	Y	Y	Y	N
Dextran-treated	Y	Y	Y	Y	Y

N indicates no binding and thus effective protein resistance. Y indicates NSB of proteins and thus poor or no protein resistance. GCD, α-glucosidase.

nanotube samples were first exposed to CDI-activated Tween (1 wt%, water) for 30 min, rinsed thoroughly with water to remove excess reagent, and then reacted with biotin-long chain-PEO-amine, SpA, or U1A (10 mM, 1 μM, and 10–100 nM, respectively) in a sodium carbonate buffer (pH 9.5) for 24 h at room temperature (4°C for U1A).

Nanotube Electronic Devices for Sensing in Solution. Devices (see Fig. 2*A*) were prepared by nanotube synthesis on 1-cm × 2-cm quartz substrates. Twenty to 50 μl of a ferritin solution (6.9 mg/ml) was deposited as a rectangular strip (1–2 mm × 10 mm) on the substrate, allowed to dry, and then calcined in air at 800°C for 5 min. The resulting discrete iron nanoparticles act as catalytic seeds for nanotube growth during subsequent chemical vapor deposition of methane to afford a layer of interconnected SWNTs (15). Metal evaporation through a shadow mask formed the final device, SWNTs bridging two Ti/Au (20/60 nm thick, electrode spacing ≈0.5–1 mm) electrodes. Sensing in solution (see Fig. 2) was carried out by monitoring electrical current through the SWNT device (resistance on the order of kiloohms) under a 10-mV bias during protein additions in 10 mM phosphate buffer solution (pH 7.0). At this low bias, control experiments revealed no appreciable ionic current through the solution.

Water-Soluble Functionalized Nanotubes. Bulk SWNTs made by high-pressure CO or laser ablation were first suspended in a 1 wt% solution of Tween 20, P103, or $C_{14}E_8$ in water by sonication for 15 min, with the final concentration of the SWNTs typically 50 μg/ml. Excess surfactant was then removed by filtration through a 0.2-μm polycarbonate membrane, after which the nanotubes were resuspended in pure water by sonication, and the process was repeated three times.

Results and Discussion

Step 1: Elucidating NSB of Proteins on Pristine SWNTs. NSB on as-grown SWNTs is found to be a general phenomenon with all proteins studied in this work, including SA, avidin, BSA, α-glucosidase, SpA, and human IgG. AFM reveals nonspecifically adsorbed proteins on SWNT sidewalls after 1 h of incubation in 10–50 nM buffered protein solutions (Fig. 1*B*). This spontaneous adsorption on carbon nanotubes is attributed to hydrophobic interactions (refs. 8, 10, 16, and 17; ref. 18 and references therein) between the protein and nanotube surface. SA, a protein known to include many hydrophobic regions on its exterior, can in fact form close-packed ordered structures on the surfaces of large diameter (≈20 nm) multiwalled nanotubes because of these hydrophobic interactions (8). Further confirmation is provided by QCM, which is used to monitor protein adsorption on dense films of SWNTs in real time. Fig. 1*C* shows decreases in the resonance frequency (indicating mass uptake by the surface) of a sample upon successive additions of protein at increasing concentrations. This NSB is irreversible, as the QCM signal does not exhibit recovery upon buffer rinsing. In control

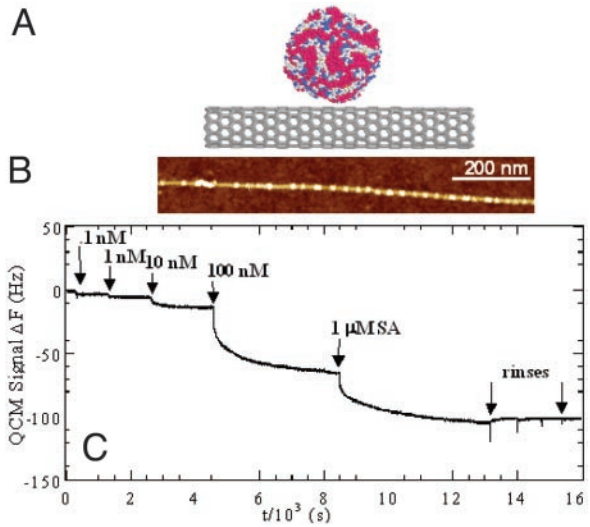

Fig. 1. Proteins tend to bind nonspecifically onto as-grown carbon nanotubes. (*A*) Schematic illustration of globular protein adsorption onto a nanotube. (*B*) An AFM image showing protein A (bright dot-like structures decorating the line-like nanotube) nonspecifically adsorbed on a nanotube. We have also observed a certain degree of NSB of proteins on regions of the (SiO_2) substrate free of nanotubes (data not shown). (*C*) QCM data (frequency shift ΔF vs. time t) revealing NSB of SA onto nanotubes at increasing protein concentrations. The NSB is irreversible upon rinsing.

experiments, we find that the degree of protein NSB on bare gold QCM substrates is a factor of ≈5 less than that on nanotube films. This finding suggests a SWNT coverage on QCM substrates of ≈90% (as estimated by comparing the differences in protein mass uptake with and without nanotubes) and that the mass uptake in Fig. 1*C* is mostly caused by protein NSB on nanotubes.

In addition to microscopy and QCM characterization, we find that nanotubes can be directly used as an electronic analytical tool to detect and monitor protein adsorption with high sensitivity. A typical electronic device is shown in Fig. 2*A*, comprising a network of SWNTs synthesized by chemical vapor deposition on discrete Fe nanoparticles (15, 19) bridging two metal (Ti/Au) electrodes. The device is immersed in a phosphate buffer solution (10 mM, pH 7.0), and its electrical conductance is monitored while proteins are added to the solution (Fig. 2*B*). The conductance (G) decreases upon stepwise exposure to SA (100 pM to 10 nM) (Fig. 2*C*); subsequent rinsing of the device does not lead to any appreciable recovery. The electronic detection data bear clear similarities to that obtained by QCM, strongly suggesting that adsorption of SA on nanotubes is responsible for the observed conductance change. With the combined approach of AFM, QCM, and electronic sensing, we obtain consistent results that reveal the generic NSB of various proteins on as-grown nanotubes (Table 1).

It is well known that SWNTs can be either metallic or semiconducting depending on their chirality (6) and that only semiconducting nanotubes exhibit a large conductance change in response to the electrostatic and chemical gating effects desired for field-effect transistors (FETs) and chemical sensors, respectively (12, 20, 21). SWNTs synthesized by our chemical vapor deposition method have been characterized as expressing a high percentage (≈70%) (19) of semiconductors that exhibit *p*-type FET characteristics in air (12, 20). Because of this high percentage, nanotubes in an interconnected submonolayer network (Fig. 2*A*, AFM image) collectively exhibit semiconductor-like behavior as evident in Fig. 2*D*, in which the conductance can be sensitively gated (22, 23) by voltages applied through a Pt

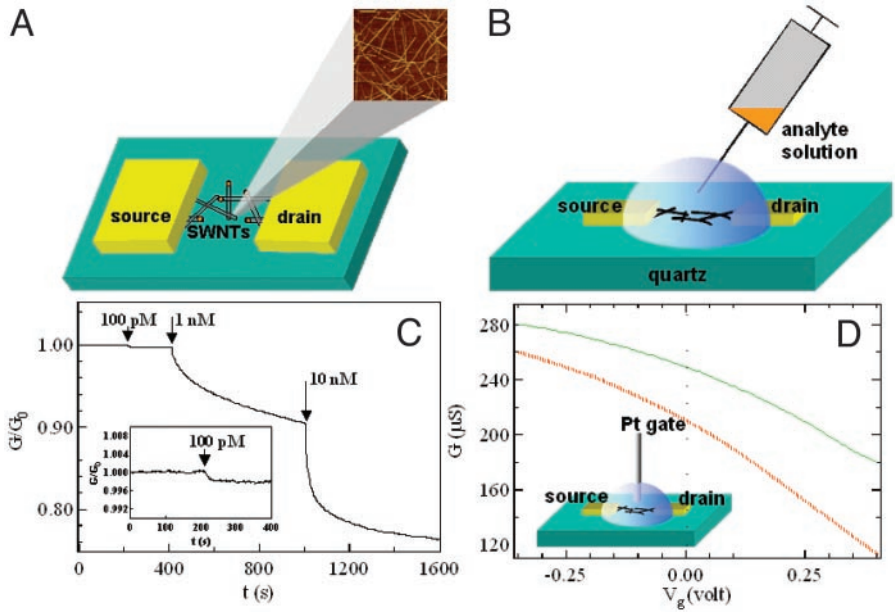

Fig. 2. Carbon nanotubes as electronic devices for sensing in aqueous solutions. (*A*) Schematic views of the electronic sensing device consisting of interconnected nanotubes bridging two metal electrode pads. An AFM image of a portion of the nanotube network (0.5 μm on a side) is shown. (*B*) Schematic setup for sensing in solution. (*C*) Conductance (G) evolution of a device for electronic monitoring of SA adsorption on nanotubes. The conductance is normalized by the initial conductance G_0. (*Inset*) Sensitivity to a 100-pM protein solution is shown. (*D*) Electrical conductance (G) vs. gate voltage (V_g) for a device in a 10-mM phosphate buffer solution. The gate voltage is applied through a Pt electrode immersed in the solution (*Inset*). The green (solid) and orange (broken) curves are the G–V_g characteristics for the device before and after SA binding, respectively. The shift in the two curves suggests a change in the charge environment of the nanotubes.

electrode immersed in a pH 7.0 buffered solution (Fig. 2*D Inset*). The conductance changes significantly upon sweeping the gate from −400 to 400 mV (Fig. 2*D*, solid curve). Similar measurement after SA binding shows a pronounced shift in the conductance vs. gate characteristics (Fig. 2*D*, broken curve). SWNT devices thus display the ability to act as FETs in aqueous solutions. Nevertheless, the precise manner by which conductance change is effected by protein binding remains to be elucidated. Although it would be expected that the binding of a positively charged protein on a SWNT would induce a conduc-

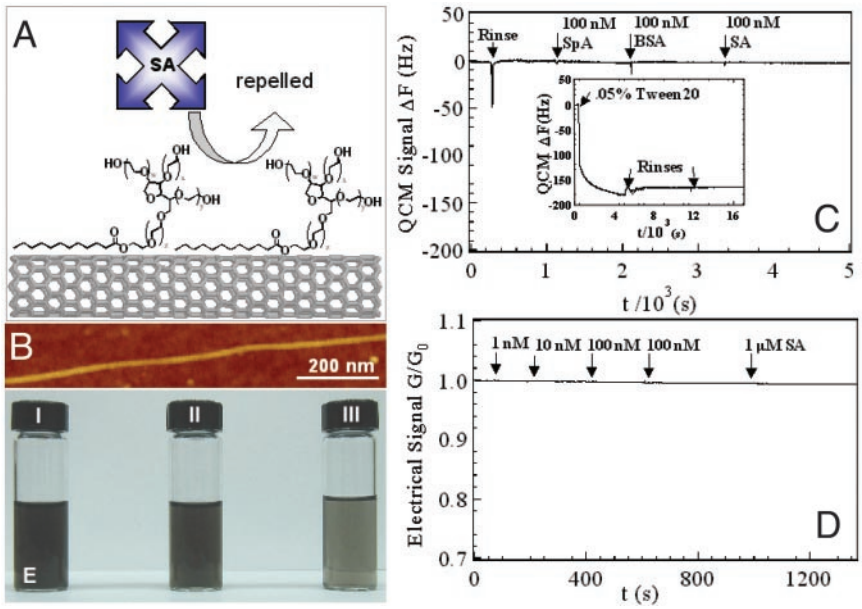

Fig. 3. Noncovalent functionalization of nanotubes for protein resistance and water solubility. (*A*) Schematic of a monolayer of Tween 20 anchored on a nanotube, repelling NSB of proteins in solution. (*B*) An AFM image showing the absence of adsorbed proteins on a Tween-coated nanotube after exposure to a 10-nM SA solution for 60 min. (*C*) QCM data showing the absence of mass uptake and thus no NSB of various proteins onto a film of Tween-coated nanotubes. (*Inset*) The irreversible adsorption of Tween onto such a film is shown. (*D*) The conductance of a Tween-coated nanotube electronic device does not exhibit any change upon exposure to various protein solutions. (*E*) Photographs that show SWNTs coated with Tween (I) and P103 (II) forming stable suspensions in water. The suspension in III is derived from $C_{14}E_8$-treated SWNTs, but to obtain a stable suspension, a lower concentration of SWNTs is necessary, resulting in a lighter-color solution than those in I and II.

tance change opposite to that of a negatively charged one, all of the proteins tested cause a decrease in conductance, regardless of the sign of the net charge (e.g., SA, pI ≈5.5, and avidin, pI ≈10; both give the same direction of change). Therefore, a mechanism by which protein provides an electrostatic gating effect does not adequately explain the observed conductance behavior. Although further work is necessary to elucidate the mechanism, the electronic signal generated by protein adsorption on SWNTs is consistently observed at the ≈100-pM level; QCM, in comparison, detects at ≈10 nM. Note that the interconnected SWNT devices used here can be grown reproducibly by chemical vapor deposition. The ensemble-averaged electrical characteristics (e.g., conductance vs. gate, Fig. 2*D*) are highly consistent from device to device and exhibit low electrical noise, features desired for sensors.

Step 2: Developing a Noncovalent Nanotube Functionalization Scheme for Protein Resistance. The second step of our work focuses on preventing protein NSB on nanotubes through noncovalent functionalization that preserves their unique electrical properties. Our approach is to immobilize PEO units on nanotube sidewalls and is motivated by the well-established protein-resisting abilities of PEO (refs. 16 and 17; ref. 18 and references therein). Of 10 PEO-containing molecules investigated, Tween 20 and a series of Pluronic triblock copolymers are found to strongly adsorb onto SWNTs and impart high protein resistance. Tween 20 is a surfactant comprising a linear aliphatic chain and three PEO branches (Fig. 3*A*). Pluronic P103 is a $(PEO)_x$–(polypropylene oxide)$_y$–$(PEO)_x$ triblock copolymer with hydrophilic PEO segments ($x \approx 20$) as well as a substantial hydrophobic polypropylene oxide block ($y \approx 52$). QCM reveals that both of these molecules spontaneously and irreversibly adsorb onto nanotubes (Fig. 3*C Inset*) from aqueous solution.

Tween- and P103-coated SWNTs exhibit excellent resistance to NSB of all of the proteins tested (Table 1) at up to 1 μM as revealed by AFM (Fig. 3*B*). QCM data likewise show no mass uptake and thus no NSB on films of similarly coated SWNTs (Fig. 3*C*). As well, no change is observed in the electrical conductance of electronic devices (Fig. 3*D*). These results suggest that PEO chains are anchored on the nanotube sidewalls with sufficient coverage and density to impart excellent resistance to protein NSB.

PEO as a protein NSB suppressant has been previously used for macroscopic substrates in the form of oligo(ethylene glycol) on silicon, gold, metal oxide, and polymer surfaces (refs. 16, 17, and 24–26; ref. 18 and references therein). These molecules render the surface highly hydrophilic and charge-neutral, thereby eliminating hydrophobic interactions and electrostatic binding with proteins (27). PEO functionalization of SWNTs is believed to operate similarly. We suggest that a nearly uniform monolayer of Tween and P103 molecules is strongly bound to the surface of SWNTs in solution. The van der Waals interaction between the hydrophobic segment of the molecules and the nanotube sidewall is robust against desorption in aqueous solutions because of favorable hydrophobic–hydrophobic association. The PEO segments, meanwhile, extend into the water and impart protein resistance to the surface (26, 28). Thus far, only Tween and P103 have been identified to impart such resistance to nanotubes. Dextran [well known for its protein-repelling properties (refs. 16 and 17; ref. 18 and references therein)] and other PEO-containing surfactants such as Triton X-100 and tetradecyloctaglycol ($C_{14}E_8$) give only poor to partial resistance (Table 1). We suggest that, along with multiple PEO chains per molecule, a largely linear hydrophobic segment, such as the aliphatic portion of Tween and the polypropylene oxide block in P103, is key to forming a densely packed, irreversibly adsorbed layer for effective NSB resistance. This finding leads to an

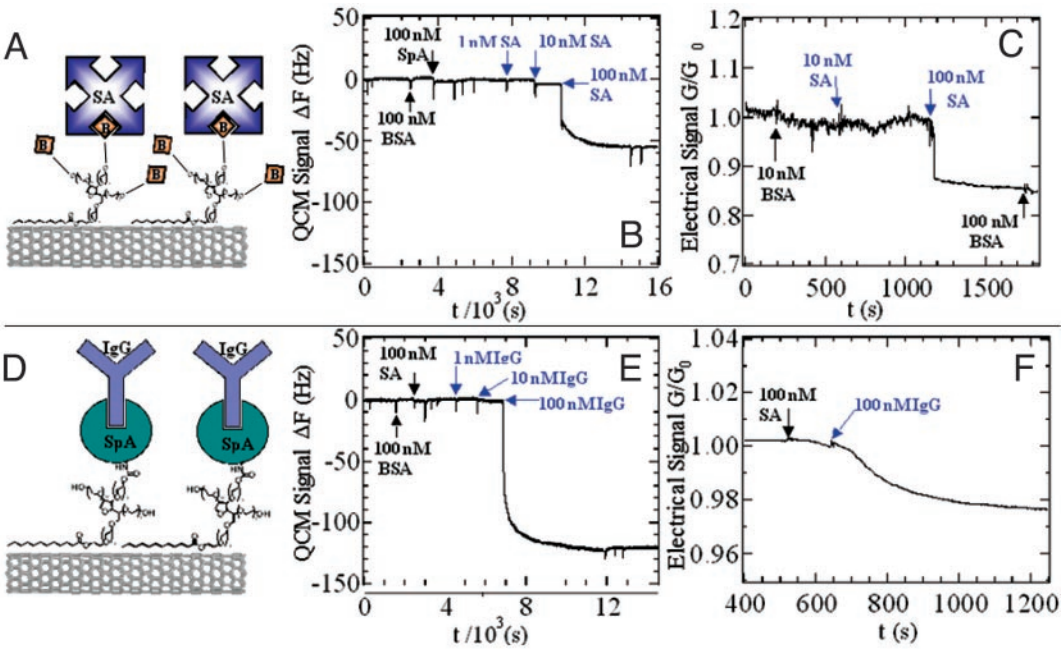

Fig. 4. Real-time QCM and electronic sensing of specific biological recognition on nanotubes. (*A*) Scheme for SA recognition with a nanotube coated with biotinylated Tween. (*B*) QCM frequency shift vs. time curve showing that a film of nanotubes coated with biotinylated Tween binds SA specifically but not other proteins. (*C*) Conductance vs. time curve of a device during exposure to various protein solutions. Specific binding of SA is detected electronically. (*D*) Scheme for IgG recognition with a nanotube coated with a SpA–Tween conjugate. (*E*) QCM frequency shift vs. time curve showing a film of nanotubes coated with SpA–Tween binding human IgG specifically but not unrelated proteins. Note that 10 nM IgG concentration approaches the lower detection limit of the instrument, whereas 100 nM approaches surface saturation of the sample; thus, the response does not show a full proportionality to the concentration. (*F*) Conductance vs. time curve of a device during exposure to various protein solutions. Specific binding of IgG is detected electronically (some NSB is observed for 100 nM SA, but the signal is much smaller than that of IgG).

extremely simple and novel functionalization approach needed for selective biosensing devices.

Robustness of Noncovalent PEO Functionalization. AFM, QCM, and electronic probe experiments reveal that for SWNTs coated with Tween or P103 excellent protein resistance persists after being immersed in pure buffer solutions for >2 weeks. Further, a high degree of resistance remains after heating coated samples in solution overnight at 60°C. Also important is that noncovalent coating by Tween and P103 imparts excellent water solubility to SWNTs. We dispersed bulk amounts of SWNTs in a Tween or P103 solution, removed the excess by filtration, and redispersed the SWNTs in pure water with slight sonication. The resulting suspensions of SWNTs (Fig. 3*E*) are stable for >7 days. Moreover, addition of phosphate buffer to the water suspension does not cause aggregation of the nanotubes. These results suggest that Tween and P103 are strongly anchored on nanotubes and do not desorb over time or at relatively high temperatures in solution.

Step 3: Selective Biological Recognition on Nanotube Devices. Tween- and P103-coated SWNTs show excellent resistance to the NSB of various proteins. The next objective then is to reenable binding to selected targets in solution by covalently linking their binding partners to the PEO-functionalized nanotubes. By so doing, only analytes exhibiting high affinity toward the tethered molecules will bind, whereas low-affinity species will be rejected. We first illustrate this selective biological recognition on nanotubes with the SA–biotin pair (dissociation constant on the order of 10^{-15} M). 1,1-Carbonyldiimidazole (29) is used to activate the hydroxyl termini of Tween toward nucleophilic addition. Nanotube samples are immersed in a solution of this activated Tween (1 wt%, water) for 30 min and rinsed thoroughly, after which biotin-long chain-PEO-amine (5–10 mM in sodium carbonate buffer, pH 9.5) is added and allowed to react for 24 h at room temperature, resulting in biotinylation of the adsorbed Tween. *In situ* QCM monitoring reveals efficient and irreversible binding of SA onto these specifically functionalized SWNTs and the absence of NSB of other species, including BSA, SpA (Fig. 4*B*), α-glucosidase, human IgG, and biotin-plugged SA (data not shown).

As well as smaller biomolecules like biotin, the hydroxyl activation chemistry allows for the general immobilization of proteins through conjugation with their lysine residues, enabling the study of specific protein–protein binding interactions with nanotube devices (Fig. 4*D*). As an example, for a Tween-coated SWNT sample to which SpA is conjugated in the same manner as described for biotin, QCM reveals large mass uptake and binding of IgG from solution (dissociation constant $\approx 10^{-7}$ M for SpA–IgG), whereas little binding is observed for proteins that do not interact specifically with SpA (Fig. 4*E*). This finding demonstrates that antigens immobilized on PEO-functionalized nanotubes retain their antigenicity and can bind their respective antibodies with high specificity.

Biological specificity, combined with the unique electronic properties of nanotubes, enables nanotube-based biosensors that can selectively detect proteins in solution by using direct electronic readout without the need for labeling. In Fig. 4*C*, we show that the electrical conductance of a nanotube device coated with biotinylated Tween exhibits an appreciable decrease upon binding SA in solution. The electronic detection is selective; no signal is detected with the same device when exposed to other proteins. In separate experiments, a nanotube device coated with an SpA–Tween conjugate exhibits specific detection with an appreciable conductance change upon exposure to IgG but not to unrelated proteins (Fig. 4*F*). Thus, specific ligand–protein and protein–protein interactions can be probed by using nanotubes directly as electronic transducers.

Building on these results, we next demonstrate nanotube biosensors for potential medical diagnostic and biological applications by attempting to detect the binding of mAbs to an immobilized, recombinant human autoantigen. U1A RNA splicing factor is a prominent autoantigen target in systemic lupus erythematosus and mixed connective tissue disease, and the detection of autoantibodies directed against this protein forms the basis for a commonly used clinical assay. This is typically carried out by standard fluorescence-based techniques, such as ELISA, which requires labeling steps to visualize binding. With nanotube sensors, binding can be monitored in real time electronically without resorting to labeling. U1A, a 33-kDa protein that forms part of the U1–small nuclear ribonucleoprotein complex, was produced in insect cells, purified, and conjugated to Tween-coated nanotube devices in the same manner as described above. Subsequent QCM (Fig. 5*B*) and electronic (Fig. 5*C*) measurements reveal selective binding of 10E3, a mAb that

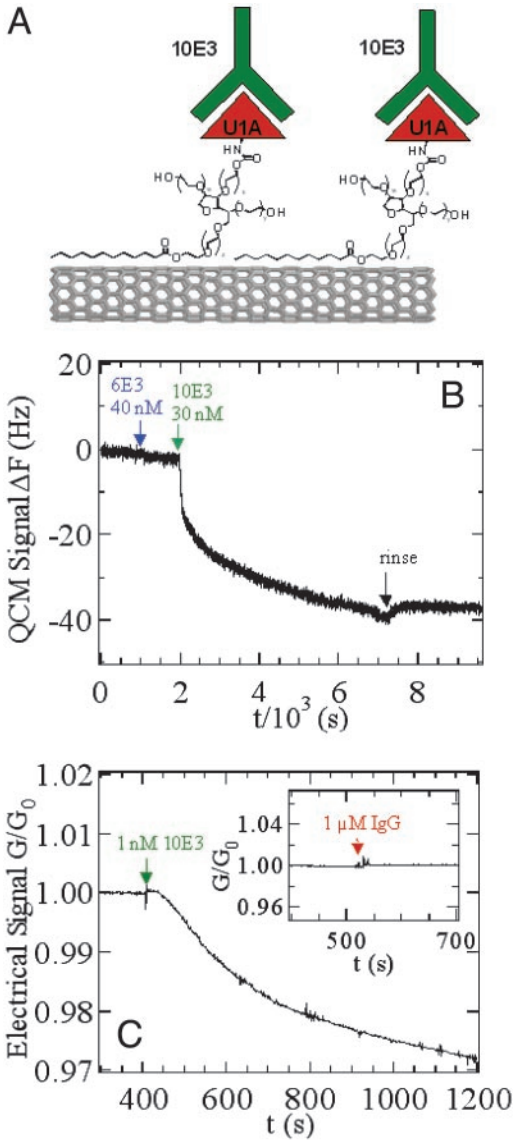

Fig. 5. Specific detection of mAbs binding to a recombinant human autoantigen. (*A*) Scheme for specific recognition of 10E3 mAb with a nanotube device coated with a U1A antigen–Tween conjugate. (*B*) QCM frequency shift vs. time curve showing selective detection of 10E3 while showing rejection of the antibody 6E3, which recognizes the highly structurally related autoantigen TIAR. (*C*) Conductance vs. time curve of a device shows specific response to ≤1 nM 10E3 while rejecting polyclonal IgG at a much greater concentration of 1 μM (*Inset*).

specifically recognizes only U1A, at concentrations ≤1 nM. Identical results were also seen with two other U1A-specific mAbs (data not shown). In contrast, two different mAbs (3E6 and 6E3) specific for a structurally related but different RNA binding protein autoantigen, TIAR (30), did not recognize U1A in this assay. This finding compares favorably with fluorescence-based detection of immobilized antigens on planar arrays, in which the limit of detection was found to be 340 ng/ml (≈2.3 nM) (31). Our current scheme also allows all sample preparation and detection to be performed in the solution phase without drying the proteins. These results demonstrate that nanotube devices can be effectively used to detect clinically and biologically important interactions between antibodies and antigens, with a potential for high throughput screening assays of mAb panels for use as reagents or even therapeutics (32). It is estimated that the human proteome contains >300,000 different protein isoforms, and methods for high-throughput screening of mAbs are badly needed for their identification. Arrays of nanotube devices could be used to perform multiplex analysis of autoantibodies to diagnose patients with autoimmune disease, complementing or perhaps replacing other recently developed techniques such as planar array-based methods (33, 34).

Conclusion and Perspectives

Exploratory research has been carried out in interfacing SWNTs with biological systems. We have demonstrated nanotube-based biosensors capable of the selective detection of proteins in solution. The present work leads to two important directions of study. The first is the utilization of nanotubes in detecting serum proteins, including disease markers, autoantibodies, and antibodies (e.g., after therapeutic interventions or vaccinations). The second is the synthesis and fabrication of high-density nanotube device microarrays (35, 36) for proteomics applications, aimed at detecting large numbers of different proteins in a multiplex fashion by using purely electrical transducers. These arrays are attractive because no labeling is required and all aspects of the assay can be carried out in solution phase. The current work establishes a foundation for this exciting application. Interfacing novel nanomaterials with biological systems could therefore lead to important applications in disease diagnosis, proteomics, and nanobiotechnology in general.

We are grateful to Professor Calvin F. Quate for insightful discussions, Professor Curtis Frank for the use of QCM equipment, and Professors Paul Anderson and Carol Lutz for the gifts of TIAR and U1A mAbs, respectively. H.D. acknowledges support from the Defense Advanced Research Planning Agency Microsystems Technology Office, a Packard Fellowship in Science and Engineering, and an Alfred Sloan Fellowship. P.J.U. acknowledges support from the Arthritis Foundation, a Baxter Foundation Career Development Award, a Bio-X grant, a Program in Molecular and Genetic Medicine grant, and National Institutes of Health Grants K08 AI01521, DK61934, AI051614-01, and AI50864-01, and National Heart, Lung, and Blood Institute Proteomics Center Contract NO1-HV-281.

1. Bruchez, M., Moronne, M., Gin, P., Weiss, S. & Alivisatos, A. P. (1998) *Science* **281,** 2013–2016.
2. Taton, T., Mirkin, C. & Letsinger, R. (2000) *Science* **289,** 1757–1760.
3. Cui, Y., Wei, Q., Park, H. & Lieber, C. (2001) *Science* **293,** 1289–1292.
4. Wong, S., Joselevich, E., Woolley, A., Cheung, C. & Lieber, C. (1998) *Nature* **394,** 52–55.
5. Chen, R. J., Zhang, Y., Wang, D. & Dai, H. (2001) *J. Am. Chem. Soc.* **123,** 3838–3839.
6. Dresselhaus, M. S., Dresselhaus, G. & Eklund, P. C. (1996) *Science of Fullerenes and Carbon Nanotubes* (Academic, San Diego).
7. Dresselhaus, M. S., Dresselhaus, G. & Avouris, P. (2001) *Carbon Nanotubes* (Springer, Berlin).
8. Balavoine, F., Schultz, P., Richard, C., Mallouh, V., Ebbesen, T. W. & Mioskowski, C. (1999) *Angew. Chem. Int. Ed.* **38,** 1912–1915.
9. Erlanger, B. F., Chen, B., Zhu, M. & Brus, L. E. (2001) *Nano Lett.* **1,** 465–467.
10. Shim, M., Wong Shi Kam, N., Chen, R. J., Li, Y. & Dai, H. (2002) *Nano Lett.* **2,** 285–288.
11. Mattson, M. P., Haddon, R. C. & Rao, A. M. (2000) *J. Mol. Neurosci.* **14,** 175–182.
12. Kong, J., Franklin, N. R., Zhou, C. W., Chapline, M. G., Peng, S., Cho, K. J. & Dai, H. (2000) *Science* **287,** 622–625.
13. Collins, P. G., Bradley, K., Ishigami, M. & Zettl, A. (2000) *Science* **287,** 1801–1804.
14. Shim, M., Javey, A., Wong Shi Kam, N. & Dai, H. (2001) *J. Am. Chem. Soc.* **123,** 11512–11513.
15. Li, Y., Kim, W., Zhang, Y. G., Rolandi, M., Wang, D. W. & Dai, H. (2001) *J. Phys. Chem.* **105,** 11424–11431.
16. Szycher, M. (1983) *Biocompatible Polymers, Metals and Composites* (Technomic, Lancaster, PA).
17. Harris, J. M. & Zalipsky, S. (1997) *Poly(ethylene glycol): Chemistry and Biological Applications* (Am. Chem. Soc., Washington, DC).
18. Ostuni, E., Chapman, R. G., Holmlin, R. E., Takayama, S. & Whitesides, G. M. (2001) *Langmuir* **17**, 5605–5620.
19. Kim, W., Choi, H. C., Shim, M., Li, Y., Wang, D. & Dai, H. (2002) *Nano Lett.* **2,** 703–708.
20. Tans, S., Verschueren, A. & Dekker, C. (1998) *Nature* **393,** 49–52.
21. Kong, J. & Dai, H. (2001) *J. Phys. Chem.* **105,** 2890–2893.
22. Kruger, M., Buitelaar, M. R., Nussbaumer, T., Schonenberger, C. & Forro, L. (2001) *Appl. Phys. Lett.* **78,** 1291–1293.
23. Rosenblatt, S., Yaish, Y., Park, J., Gore, J., Sazonova, V. & McEuen, P. L. (2002) *Nano Lett.* **2,** 869–872.
24. Feldman, K., Hahner, G., Spencer, N. D., Harder, P. & Grunze, M. (1999) *J. Am. Chem. Soc.* **121,** 10134–10141.
25. Zhang, M., Desai, T. & Ferrari, M. (1998) *Biomaterials* **19,** 953–960.
26. Lee, S. W. & Laibinis, P. E. (1998) *Biomaterials* **19,** 1669–1675.
27. Holmlin, R. E., Chen, X., Chapman, R. G., Takayama, S. & Whitesides, G. M. (2001) *Langmuir* **17,** 2841–2850.
28. Schwendel, D., Dahint, R., Herrwerth, S., Schloerholz, M. Eck, W. & Grunze, M. (2001) *Langmuir* **17,** 5717–5720.
29. Hermanson, G. (1996) *Bioconjugate Techniques* (Academic, San Diego), pp. 615–617.
30. Taupin, J. L., Tian, Q., Kedersha, N., Robertson, M. & Anderson, P. (1995) *Proc. Natl. Acad. Sci. USA* **92,** 1629–1633.
31. Haab, B. B., Dunham, M. J. & Brown, P. O. (2001) *Genome Biol.* **2,** 0004.1–0004.13.
32. McCune, S. L., Gockerman, J. P. & Rizzieri, D. A. (2001) *J. Am. Med. Assoc.* **286,** 1149–1152.
33. Robinson, W. H., DiGennaro, C., Hueber, W., Haab, B. B., Kamachi, M., Dean, E. J., Fournel, S., Fong, D., Genovese, M. C., Neuman De Vegvar, H. E., *et al.* (2002) *Nat. Med.* **8,** 295–301.
34. MacBeath, G. & Schreiber, S. L. (2000) *Science* **289,** 1760–1763.
35. Franklin, N. R., Li, Y., Chen, R. J., Javey, A. & Dai, H. (2001) *Appl. Phys. Lett.* **79,** 4571–4573.
36. Qi, P., Vermesh, O., Grecu, M., Javey, A., Wang, Q., Dai, H., Peng, S. & Cho, K. J. (2003) *Nano Lett.* **3,** 347–351.